Modeling Watershed Response in Semi-Arid Regions with High Resolution Synthetic Aperture Radars

Donato Amitrano, Fabio Ciervo, Gerardo Di Martino, *Member, IEEE,* Maria Nicolina Papa, Antonio Iodice, *Senior Member, IEEE,* Youssouf Koussoube, Francesco Mitidieri, Daniele Riccio, *Fellow, IEEE,* Giuseppe Ruello, *Member, IEEE*

This work has been published on
IEEE Journal of Selected Topics in Applied Earth Observations and Remote Sensing

Abstract

In this paper we propose a methodology devoted to exploit the outstanding characteristics of COSMO-SkyMed for monitoring water bodies in semi-arid countries at a scale never experienced before. The proposed approach, based on appropriate registration, calibration and processing of Synthetic Aperture Radar (SAR) data, allows outperforming the previously available methods for monitoring small reservoirs, mainly carried out with optical data, and severely limited by the presence of cloud coverage, which is a frequent condition in wet season. A tool has been developed for computing the water volumes retained in small reservoirs based on SAR-derived digital elevation model. These data has been used to derive a relation between storage volumes and surface areas which can be used when bathymetric information are unavailable. Due to the lack of direct measures of river's discharge, the time evolution of water volumes retained at reservoirs has been used to validate a simple rainfall-runoff hydrological model which can provide useful recommendation for the management of small reservoirs. Operational scenarios concerning the improvement of the efficiency of reservoirs management and the estimation of their impact on downstream area point out the applicative outcomes of the proposed method.

Index Terms

Synthetic Aperture Radar, Small Reservoirs, Semi-arid regions

I. Introduction

In semi-arid regions, small reservoirs are widely employed for facing water scarcity and climatic variability [1], [2]. In Sub-Saharian Africa they are used for water harvesting in the rainy season and water storage in the dry season. In Burkina Faso, it is estimated that almost 1700 small reservoirs are actually used for irrigation, livestock, and other uses. Despite of their crucial importance, small reservoirs are not appropriately monitored and in many cases they are not catalogued or the relative data are not kept up-to date [2]. This is mostly true in low-income countries, and in particular in Sub-Saharian Africa. Moreover, small reservoirs are often built or modified for the initiative of local communities and even basic data as their location and capacity are not available. For these reasons it is extremely hard to study the impact of reservoirs on the territory and to optimize their management.

In order to improve the management of water supply it is necessary to provide hydrological models suitable for the specic environments under study. In literature there is a lack of environmental and hydrological data concerning semi-arid West Africa. Therefore, it is necessary to improve the data availability through the development of cost-effective monitoring techniques and to adapt the hydrological modeling to the limited available data.

The use of remote sensing in this context could really be a breakthrough, allowing dramatic reduction of costs and time needed for achieving crucial information for effective and integrated water management [3]. So far, the use of multi-spectral [4], [5] and low-resolution radars [6], [7] for reservoir monitoring evidenced great potentialities, but also poor practical results. The main limit for a continuous monitoring with passive sensors (i.e. optical sensors) turned out to be the dependence of the results on the cloud cover, which is particularly severe in wet season. Conversely, SAR systems are independent of illumination and (in particular those operating at microwave frequencies) atmospheric conditions [8]. In fact, for an X-band system like COSMO-SkyMed, the atmosphere is quite transparent, at least for intensity measurements and in absence of severe weather events [9]. Phase information, instead, could be subject to major distortions, as discussed in [10].

In the recent past, the use of SAR systems for monitoring water bodies has been mainly constrained by the limited resolution of the available sensors [11], [12] and by the fact that the interpretation of SAR images is not easy for non-expert users [13],

Fabio Ciervo, Francesco Mitidieri and Maria Nicolina Papa are with the Department of Civil Engineering, University of Salerno, Salerno Italy

Youssouf Koussoube is with the Laboratoire d'hydrogologie - Unité de formation et de recherche en Sciences de la vie et de la terre, University of Ouagadougou, Ouagadougou, Burkina Faso

Donato Amitrano, Gerardo Di Martino, Antonio Iodice, Daniele Riccio and Giuseppe Ruello are with the Department of Electrical Engineering and Information Technology, University of Napoli Federico II, Napoli, Italy.

[14]. In fact, the low spatial resolution of the previous sensor generation allowed only applications on regional scale, principally oriented on flood monitoring of wide water surfaces. Martinez and Le Toan [15] used multitemporal SAR data for studying flood dynamics in the Amazon floodplan. Tholey *et al.* [16] fused SAR with exogenous and historical data for flood monitoring and prevention purposes. More recently, data acquired by COSMO-SkyMed, the constellation of the Italian Space Agency, powered this kind of applications thanks to the high resolution and the short revisit time that the new sensors generation can offer to the scientific community [17]. Indeed, the literature about small reservoirs monitoring is still related with the past sensor generation. In fact, references [11], [18], [19] indicated as small reservoirs water surfaces smaller than 100 hectares. This is almost at the limit of the imaging capability of the sensors used in those investigations. The introduction of the COSMO-SkyMed high resolution capabilities can strongly reduce the dimension of the observable surfaces allowing studying basins with extension in the order of few thousand square meters. In addition, the limited land-water contrast and the presence of vegetation (reeds on the reservoir tails) further hampered the accuracy of the estimation of the presence of water bodies. Misclassification and underestimation of the available volumes are typical problems in the identification of surface water.

In this paper, we present a flexible, multidisciplinary and user-friendly approach for exploiting the new possibilities born with the launch of COSMO-SkyMed for monitoring water bodies. It is flexible because it is made of interchangeable modules that can be adapted to physical or economical needs dictated by the context. It is multidisciplinary because it combines remote sensing and hydrological models and tools in order to complete their strengths. It is user-friendly because it is not limited to the creation of SAR products; it provides new products that can be easily read and used by users that do not have a background on SAR remote sensing. These characteristics allow going beyond most of the existing limits, opening the way to new fields of applications that could provide humanitarian, technological and economic benefits.

The proposed approach is supported by the results obtained in the frame of the WARM project developed in northern Burkina Faso (a landlocked country characterized by a semi-arid climate) under the aegis of the 2007 Italian Space Agency Announcement of Opportunity for the scientific use of COSMO-SkyMed data "Use of high resolution SAR data for water resource management in semi arid regions" [20] during which, by exploiting the peculiar local climate, we were able to retrieve topographic information with unprecedented details [21].

The overall methodology is presented in Section II. For sake of clarity, the SAR and the hydrological processing are dealt with separately, in SectionIII and Section IV, respectively. In particular, in Section III, we present the SAR processing, mainly devoted to extract topographic information and the presence of water bodies in the observed area, and we show that the combination of the obtained information leads to estimate the available water volume at the date of acquisition. The proposed procedure is cheaper and quicker than the expensive bathymetric surveys or approximate empiric methods so far used.

In Section IV the hydrological model is presented. In particular, we showed how it is possible to extract an empirical relationship between the areas and volumes of the observed reservoirs from SAR products. In addition, a model of runoff is developed and validated with the data extracted by the multitemporal set of SAR images. Examples of possible applications of the model to water management are also reported in Section IV-C.

II. Methodology and case study characterization

The study area (see Fig. 1) is located in the northern Burkina Faso, in the Yatenga province, and it is entirely enclosed in the Volta basin ($13°47'50''N, 2°23'31''W$). The region is characterized by a semi-arid climate, with precipitation concentrated in the June-September rainy season, which annually range between 500 mm (in the North) and 1000 mm (in the South). This climate calls for appropriate strategies for water storage in the rainy season and water use in dry season.

One of the oldest and most popular technique for water harvesting is the construction of dams that create small reservoirs. The northern Burkina Faso is characterized by an increasing demographic pressure and by soils that are prone to erosion, causing a sedimentation phenomenon that reduces the available water volume [22]. Many reservoirs have been built during the drought occurred between 1974 and 1987 [2], witnessing the importance that this practice assumes to face water shortages. The number of reservoirs frequently changes, due to uncontrolled construction and ruptures, so that an updated inventory of the existing reservoirs with traditional techniques is hard to obtain. The monitoring of the reservoirs would be of great importance in order to optimize their management and also because their effects on the overall water distribution of the Volta basin is still unclear and it is object of controversies with neighboring countries.

In this project, a set of 15 stripmap (3m resolution) COSMO-SkyMed images has been acquired. The data cover a temporal interval of almost one year and a half, including two rainy seasons, and are HH polarized, also for increasing the ratio between land and water reflectivity. The block diagram presented in Fig. 2 describes the overall methodology, from the input data through the proposed processing toward the expected output. More details on each block are provided in the following sections. It is worth to note that the modularity of the approach allows choosing the most appropriate technique in accordance with the desired results and the working environment. In this paper, most of the choices have been dictated by the need to obtain accurate results with the simplest techniques. Along with the obtained products, in the last column of the block diagram, a set of applications have been cited for showing the potentiality of the approach.

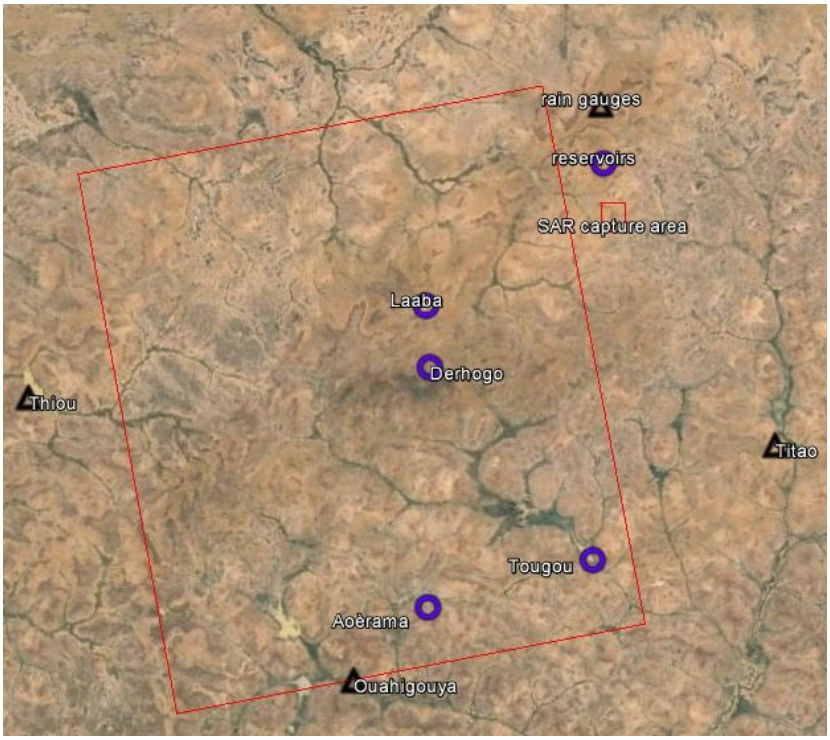

Fig. 1: Study area, Google Earth view.

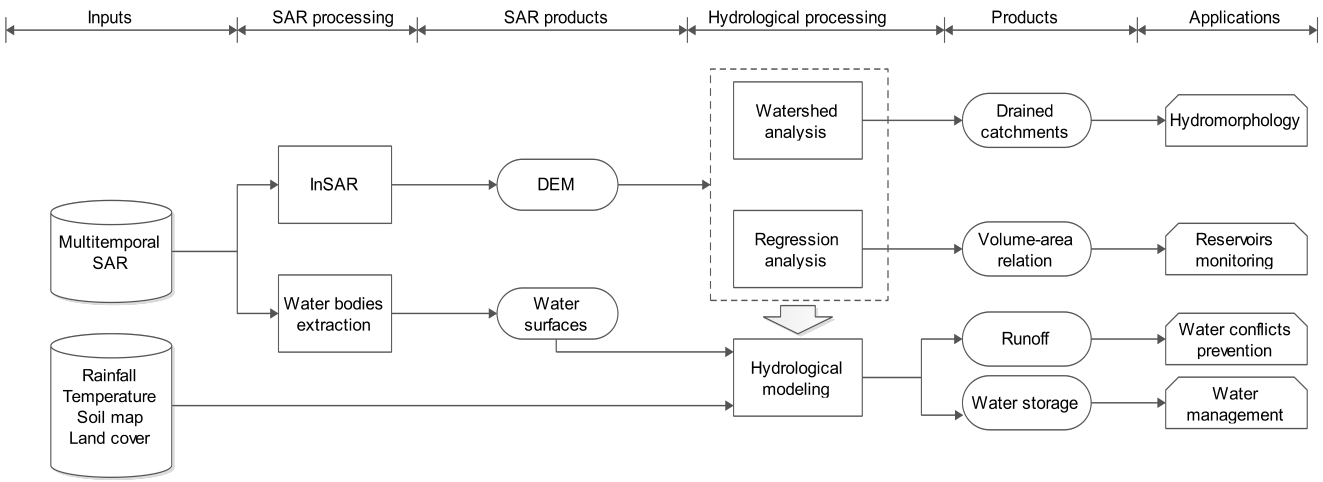

Fig. 2: Block diagram of the proposed processing chain.

III. SAR PROCESSING

In this section, we present the rationale and the algorithms developed for the estimation of the available water volumes in the monitored reservoirs. The 9 meter resolution DEM used for the bathymetric analysis was presented in [21] along with the technique employed for its generation. In particular, it was obtained processing a COSMO-SkyMed interferometric couple acquired on 2011, April 28 and 2011, April 29, at the peak of the dry season when most of the basins are empty and the climatic conditions are very stable. These conditions allow a reliable estimate of elevation and shape of the basins' areas that are covered by water in the rainy season.

A. Pre-processing

In order to exploit the temporal diversity of the SAR images, calibration, registration and despeckling procedures are required.

According to [23], COSMO-SkyMed SLC balanced products have an absolute radiometric calibration accuracy smaller than 1 dB. However, this requires the application of metadata-based calibration coefficients to the intensity map which compensate

the effects relative to the sensor and to the acquisition geometry. The procedure to be followed to correctly determine these coefficients is explained in [24].

Reduction of speckle is a fundamental aspect in multitemporal SAR processing, since its presence could complicate the identification of a relevant feature and its temporal evolution [25]. In this paper, we adopted the optimal weighting multitemporal De Grandi filter [26], which allowed us to amplify the water-land contrast and, as a consequence, to produce more accurate water-area information. A further speckle reduction has been carried out with a spatial multilooking which reduced the images' resolution to 9 meters, in accordance with the resolution of our DEM, which is the bottleneck of the whole technique.

B. Water bodies extraction

1) Segmentation: The application of the multitemporal De Grandi filter allows the enhancement of the land-water ratio and, as a consequence, an effective extraction of the shorelines by applying an intensity threshold to separate the class "water" from the class "no water" [27]. The selection of the threshold value is guided by the evaluation of the histogram of a subset taken around the basins under analysis. The constrain to respect is the selection of a subset in which the presence of surface water is relevant, since in this case the histogram of the intensity map exhibits a bimodal distribution.

In Fig. 3a we considered a subset around the Gouinre basin, whose histogram is depicted in Fig. 3b. It can be appreciated that, thanks to the multitemporal despeckling, low reflectivity objects are well-separated from the rest of the scene and this makes the image pdf bimodal. Note that this distribution emerges after an appropriate histogram clipping. In fact, Fig. 3b shows the histogram relevant to the values below the 98^{th} percentile of the pdf. This value has been selected with an entropy-guided criterion as detailed in [13], [28]. This representation allows an easy identification of the optimal threshold, which is given by the local histogram minimum between the two distribution modes. This threshold is basin- and image-adapted, since water surfaces are not necessarily static objects and their reflectivity could be influenced by local phenomena [29].

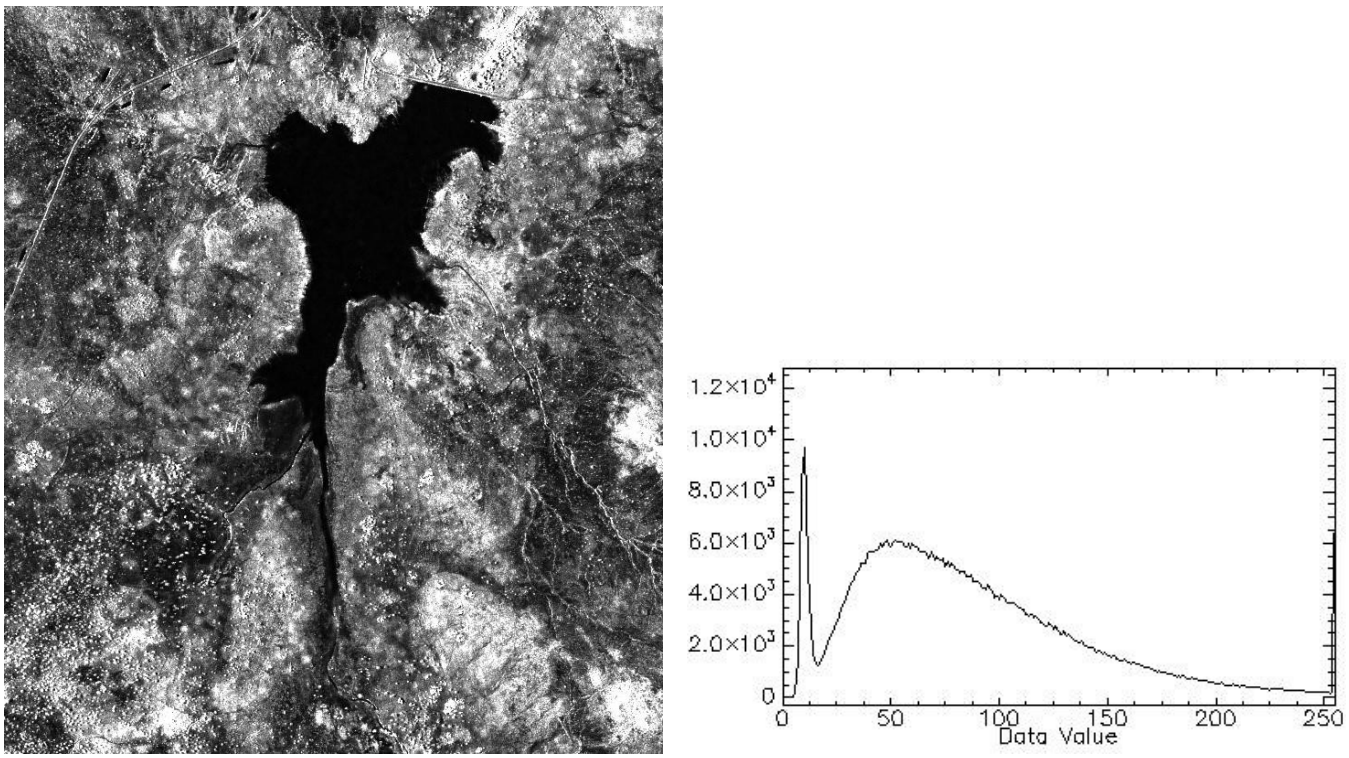

(a) (b)

Fig. 3: Gouinre basin intensity map (a) and its 98^th percentile histogram (b).

2) Shoreline extraction: The threshold-guided segmentation allows a quick preliminary estimate of the water surface [30], as shown in the example depicted in Fig. 4, where we present the SAR image of the Laaba basin (Fig. 4a) and the binary mask (Fig. 4b) obtained with the procedure presented in Section III-B1. The quality of the mask can be significantly improved, eliminating isolated pixels belonging to the "eroded areas" class [31] and wrongly classified as "water surface" with the application of a mode filter (Fig. 4c) and the use of morphological operators (Fig. 4d) [32]. Then, the shoreline is extracted with the Roberts operator (Fig. 4e) [33]. The result of the whole processing chain is shown in Fig. 4f, where a good matching between the extracted shoreline and the intensity map can be appreciated.

The extraction of the shorelines has been performed with such a semi-automatic procedure for all the available acquisition for two basins in the nearby of the city of Ouahigouya and the basins of Laaba, Tougou, Aorama, Derhogo for a total of six sites. The results of this procedure are shown in Fig. 5 to Fig. 6 for Laaba, Derhogo and Tougou basins, respectively.

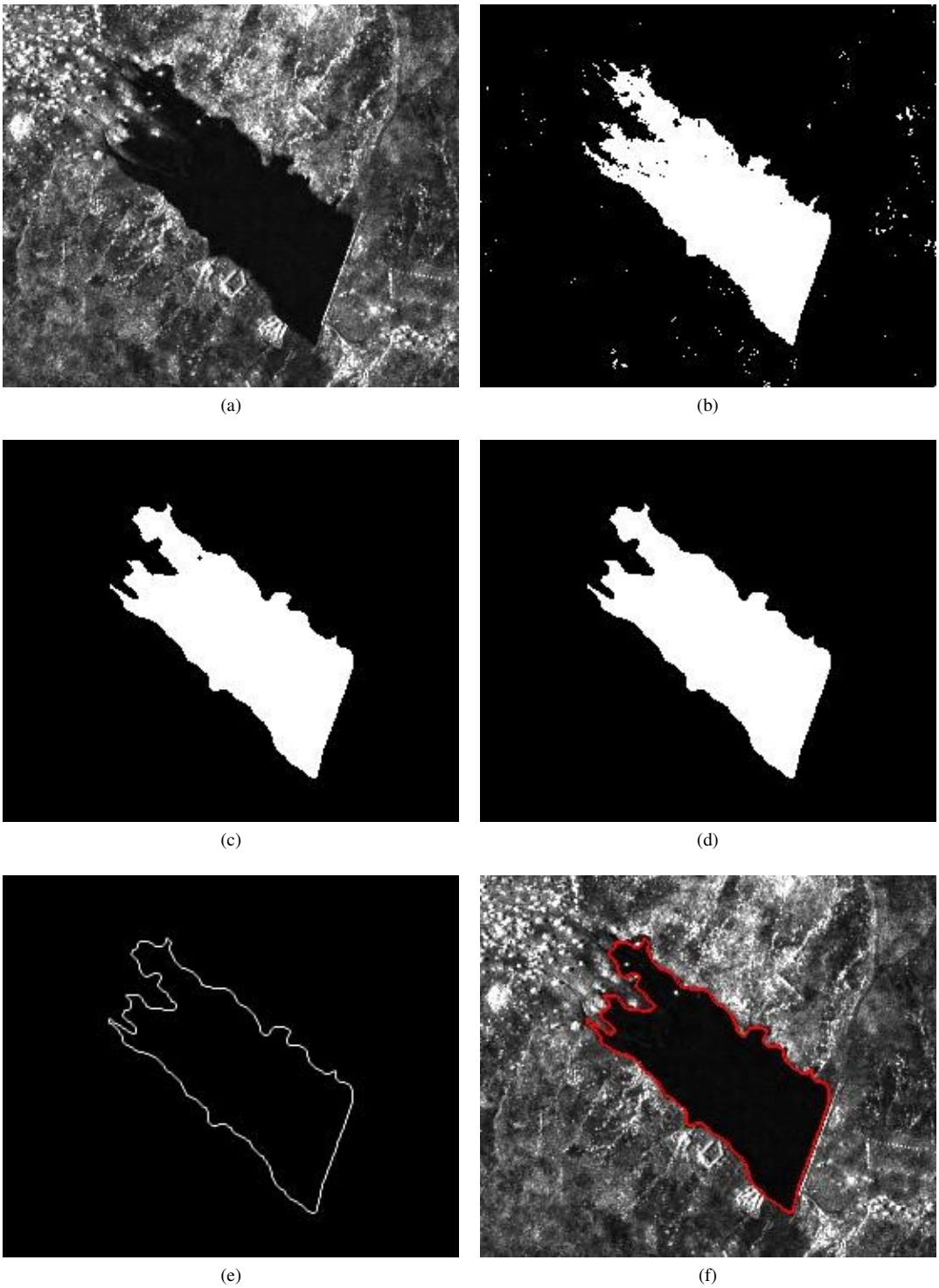

(a) (b) (c) (d) (e) (f)

Fig. 4: Shoreline extraction workflow: intensity De Grandi-filtered map (a), threshold-guided segmentation (b), mode filter (c), morphological filtering (d), Roberts edge detector (e) and superposition of the contour line on the intensity map (f).

C. Geocoding

The extracted masks and contours must be re-projected from the SAR azimuth/slant range geometry in a cartographic system through a geocoding operation. This operation is carried out through an iterative solution of the Range-Doppler equations

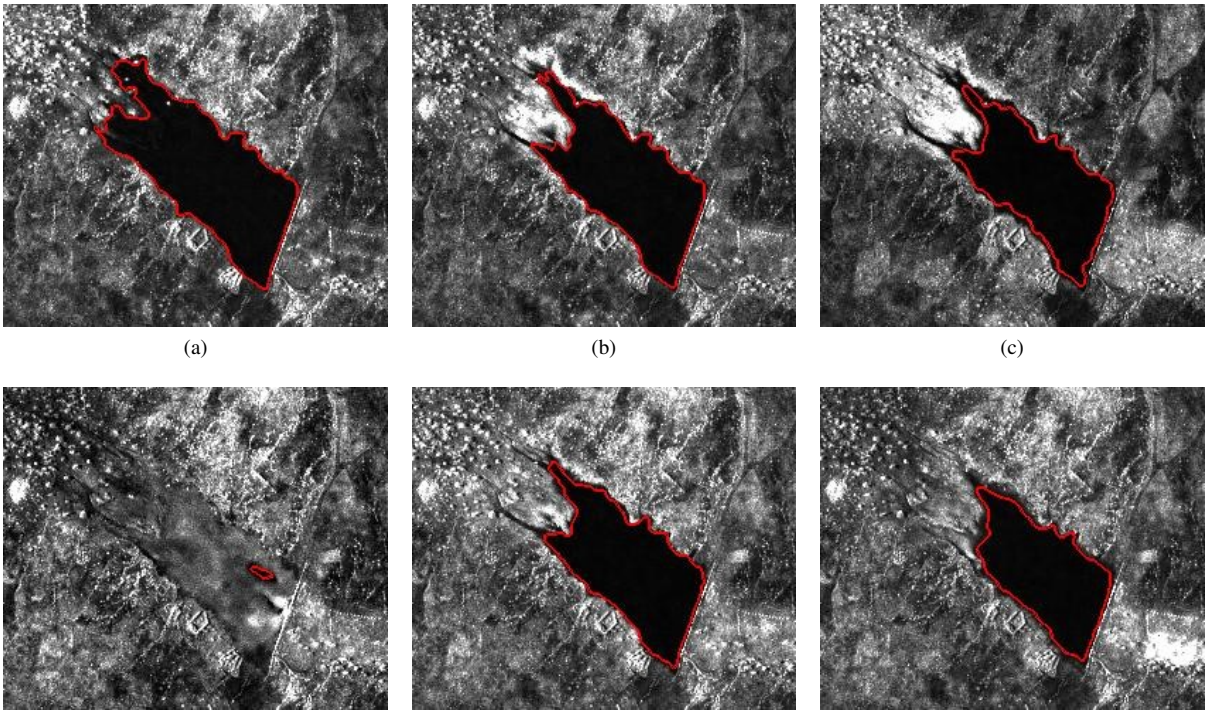

(a) (b) (c)

(d) (e) (f)

Fig. 5: Laaba basin, shorelines for the acquisitions of 2010/06/12 (a), 2010/07/14 (b), 2010/08/31 (c), 2011/03/27 (d), 2011/11/10 (e), 2011/12/12 (f).

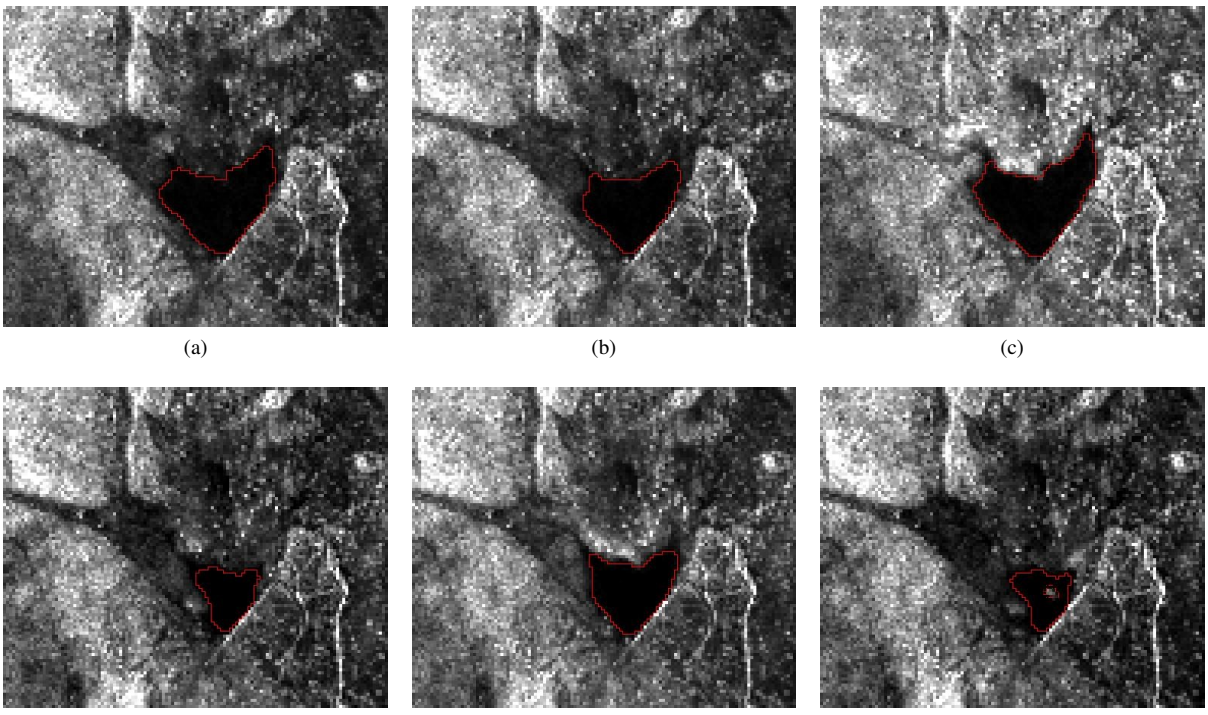

(a) (b) (c)

(d) (e) (f)

Fig. 6: Derhogo basin, shorelines for the acquisitions of 2010/06/13 (a), 2010/07/14 (b), 2010/08/31 (c), 2010/12/05 (d), 2011/11/10 (e), 2011/12/12 (f).

coupled with an Earth model for the point $\underline{\mathrm{P}} = (X, Y, Z)$ [34]. Neglecting the Earth's rotation velocity, the equations to be solved are:

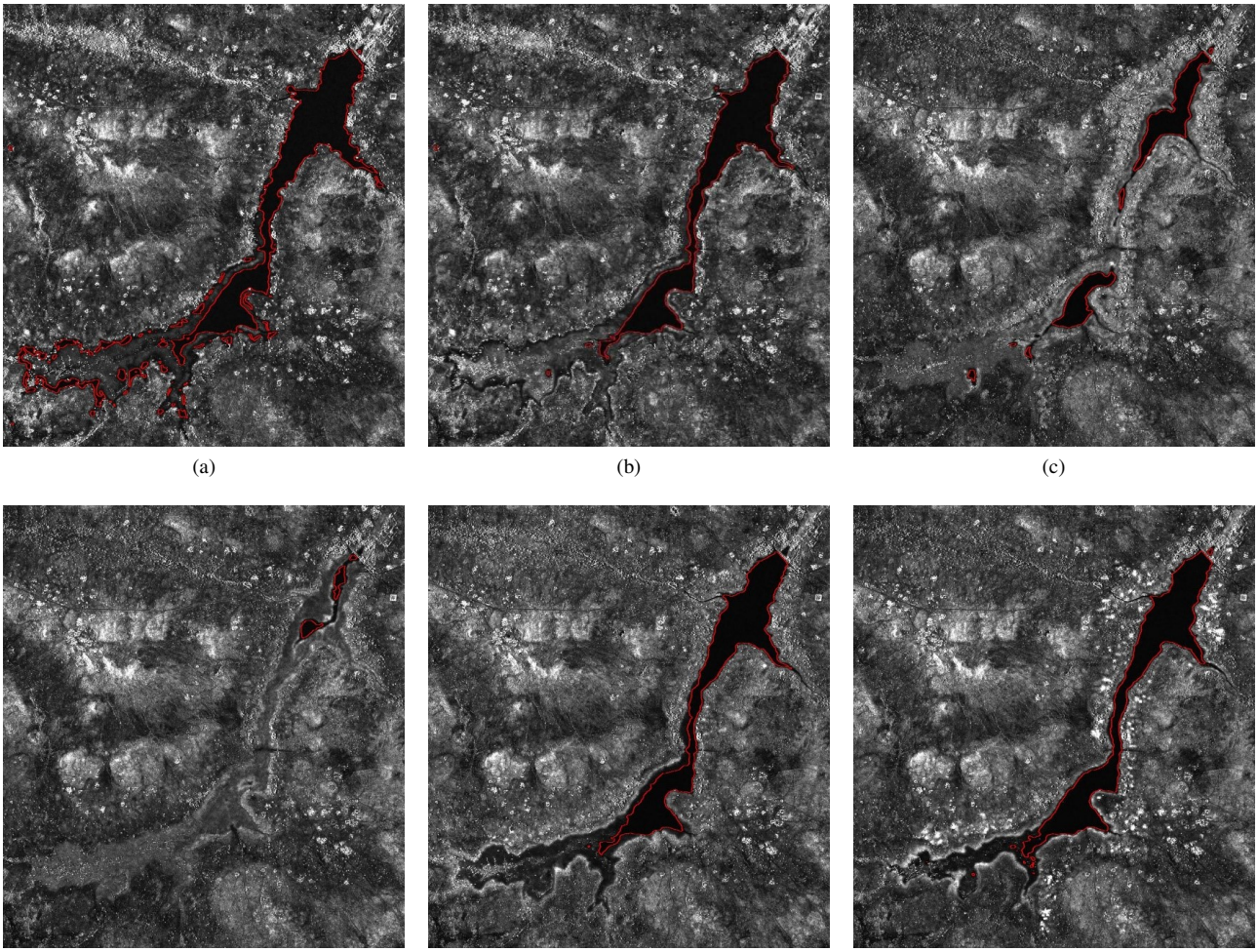

(a) (b) (c)

(d) (e) (f)

Fig. 7: Tougou basin, shorelines for the acquisitions of 2010/06/13 (a), 2010/07/14 (b), 2011/03/27 (c), 2011/04/28 (d), 2011/11/10 (e), 2011/12/12 (f).

$$(\underline{\mathrm{S}}(t_a) - \underline{\mathrm{P}}) \cdot \dot{\underline{\mathrm{S}}}(t_a) = 0 \qquad \text{(Doppler equation)} \tag{1a}$$

$$|\underline{\mathrm{S}}(t_a) - \underline{\mathrm{P}}| = t_r \frac{c}{2} \qquad \text{(Range equation)} \tag{1b}$$

$$\frac{|\underline{\mathrm{P}} \cdot \hat{e}_x|^2}{(a+h)^2} + \frac{|\underline{\mathrm{P}} \cdot \hat{e}_y|^2}{(a+h)^2} + \frac{|\underline{\mathrm{P}} \cdot \hat{e}_z|^2}{(b+h)^2} = 1 \qquad \text{(Earth model),} \tag{1c}$$

where $\underline{\mathrm{S}}$ is the satellite position, t_a the azimuth time, c the light speed, t_r the range time, $(\hat{e}_x, \hat{e}_y, \hat{e}_z)$ the unit vectors of the orbit reference system, a, b the semi-major and semi-minor axis of the ellipsoid and h is the height of the guess point with respect to the ellipsoid.

D. SAR post-processing: basins' bathymetry

Once the basin contour is known and re-projected in a cartographic system, the water volume contained into the basin can be computed considering each pixel of the water mask as a water column whose height h_{wc} is given by:

$$h_{wc} = h_c - h \tag{2}$$

where h_c is the elevation of the equipotential surface identified by the basin contour derived from the SAR intensity maps, and h is the DEM height corresponding to the considered pixel. Therefore, the water volume contained into the basin is given by the summation of all the elementary contributions brought by the water columns:

$$V = \sum_{i=1}^{N} S_i \times h_{wc_i} \tag{3}$$

where S_i is the basin surface of the $i-th$ resolution element belonging to the water mask and N is the number of pixels belonging to the water mask.

E. Analysis of the results

Figure 8 shows the results of our analysis for the six considered basins. As widely discussed in the following section, these diagrams are strictly related to the seasonal variation of rainfall with an abrupt increment of volume at the beginning of the rainy season and a continue decrease in the dry season.

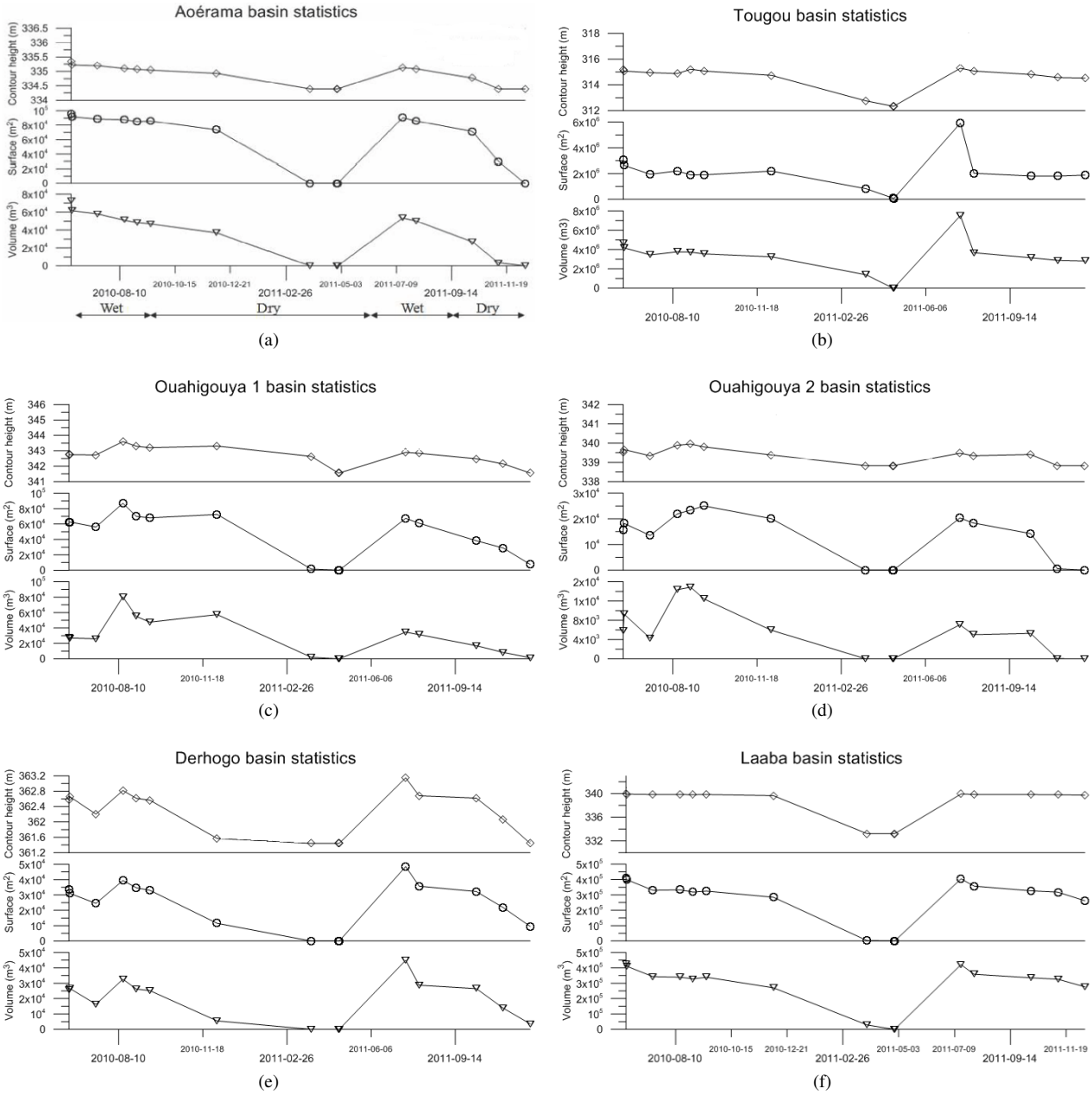

Fig. 8: Basins statistics.

Note that the Tougou basin does not dry up completely during the dry season (see Fig. 7d) and hence its bathymetry can not be estimated in the part of the basin covered by surface water during the acquisitions used for DEM retrieval. Indeed, the DEM elevation for this points is not trustworthy (due to incoherence of water surfaces return) and, therefore, they have been

excluded from the analysis using a coherence-derived mask. As a consequence, while the basin surface is correctly determined, the estimated volume represent the variation with respect to the minimum and not the entire water volume available.

In TABLE I the position of the dams and basins maximum surface and volume availability are provided. Note that also the dams' heights could be potentially estimated using the available DEM: however, typical dam's sizes in the study area are comparable to (and frequently lower than) DEM's 9 meters resolution. Hence, in most cases, the dam height estimates obtained using the DEM are not reliable. Anyway, this information is not necessary for the calculation of the retained volume. Indeed, it would be needed for the estimation of the maximum retainable volume, which is one of the inputs of the hydrological model. Nevertheless, due to the the poor quality of the dam height estimates, we assumed that the maximum retainable volume is equal to the maximum retained volume observed from SAR data, as detailed in Section III-B1 and III-D.

TABLE I: Reservoirs database.

Reservoir	Position	Surface max (m^2)	Volume max (m^3)
Laaba	$13°52'23.12''N, 2°.20'44.12''W$	407430	427215
Tougou	$13°40'48.68''N, 2°12'52.72''W$	5918022	7511779
Ouahigouya 1	$13°36'21.44''N, 2°24'42.31''W$	86994	80286
Ouahigouya 2	$13°37'78.96''N, 2°24'57.97''W$	25029	14871
Aorama	$13°40'10.61''N, 2°21'4.66''W$	96147	72723
Derhogo	$13°49'36.53''N, 2°20'34.15''W$	48519	44954

IV. Hydrological models

A. Estimation of reservoirs storage volumes as a function of their surface areas

A relation between reservoirs' storage volumes and surface areas can be derived using the obtained database. These relations are very useful since the reservoirs' surface areas can be always estimated with an excellent precision degree by satellite or aerial imagery, while the volume measurement requires more demanding and expensive bathymetric surveys.

Theoretical and empirical area-volume relations have been developed in literature, both theoretically and empirically. Based on an extensive bathymetric survey in Upper East Region of Ghana, Liebe *et al* [4] obtained the following relationship:

$$\text{Volume} = 0.00857\text{Area}^{1.4367} \ \left[m^3\right] \tag{4}$$

The regression analysis of the reservoirs volumes and areas obtained using SAR-derived data allowed the derivation of the following relation:

$$\text{Volume} = 0.10120\text{Area}^{1.1670} \ \left[m^3\right] \tag{5}$$

The Tougou basin was not used in this derivation since, as explained in Section III-E, it does not dry up completely, thus preventing the DEM extraction for the areas covered by surface water.

As shown in Fig. 9, there is only a slight difference between (4) and (5). This confirms that, thanks to the morphological and morphometrical regularity of the regions, the area-based volume estimation is possible with good approximation.

B. Modelling the time evolution of water storage

The time evolution of the water storage is computed by the implementation of a water balance among the water flows that enter and exit the reservoir. The Input flow is the surface runoff, while the outputs are the evaporation from the reservoir, the spill downstream the dam and the water withdrawn by the users. In order to validate the model, the computed storages are compared to those extracted from SAR data. The overall procedure is depicted in Fig. 10.

The first step of the model is the estimation of the runoff water that inflow the reservoir. The natural process of runoff formation is extremely complex because it is the result of many different phenomena regarding atmosphere, soil, vegetation and water flows. In literature, many hydrological models that simulate the transformation of rainfall input into surface runoff with different levels of complexity, data requirement and computational burden are available. In our case, the choice of the more appropriate hydrological modeling is mainly driven by the available (rather scarce) dataset, i.e. daily measurements of rainfall and temperature and low-resolution maps of soil and land cover. As is often the case, especially for small basins in low-income countries, run-off measurements, to be used for model calibration and validation, were not available. The lack of runoff measures is partly compensated by those of water volumes retained at the reservoirs. Due to the small number of SAR acquisitions (15 images) and the low temporal resolution, we can observe only the cumulate of the flow discharge over a period much longer than the one day time-step of the hydrological model. Consequently, the cumulate observed flow discharge cannot be used to calibrate one or more parameters of complex hydrological models. Hence, a simple hydrological model that

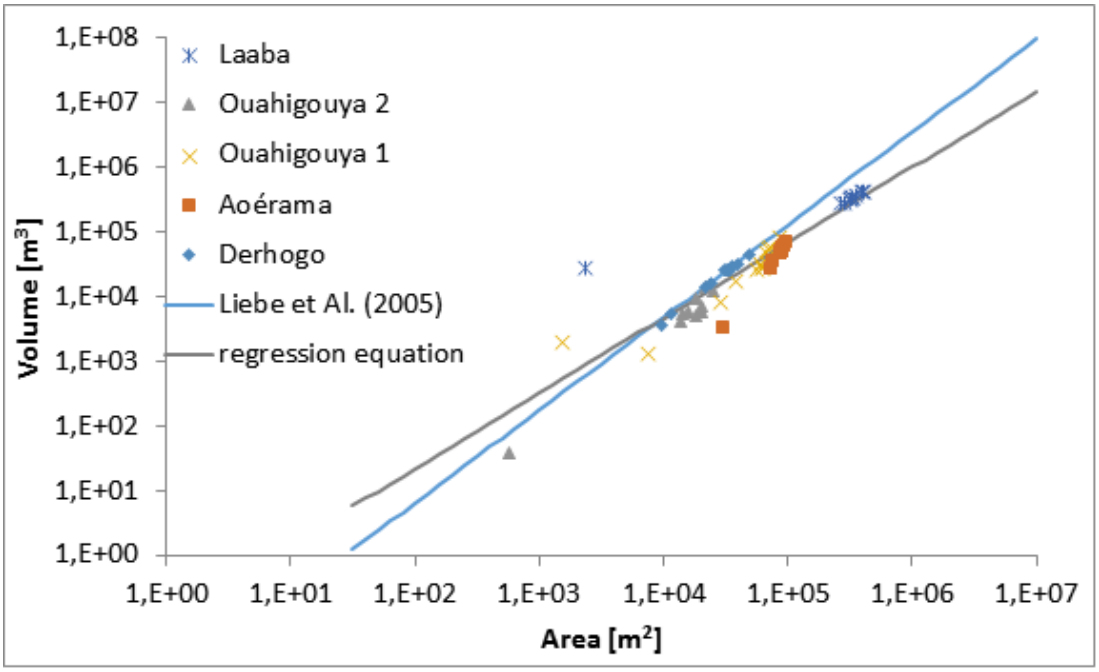

Fig. 9: Reservoirs' storage volumes as a function of their surface areas in a log-log plane.

does not require any calibration was chosen, and the retained water volumes were only used for the validation of the model. It is worthwhile to underline that denser series of SAR images would allow the calibration of more complex models that could better represent the real hydrological response.

Among the models suitable for the simulation of runoff in small ungauged watersheds which do not require the calibration of the used parameters, we used the Soil Conservation Service Method (SCS) [35]–[37], according to which the depth of runoff is given by:

$$R = \frac{(P - I_a)^2}{P - I_a + S}, \tag{6}$$

where P is the total precipitation, S the potential maximum retention and I_a the initial abstraction given by:

$$I_a = \lambda S, \;\; \lambda = 0.1 \div 0.2\,. \tag{7}$$

The potential maximum retention S is expressed in the form of a dimensionless runoff curve number CN:

$$S = S_0 \left(\frac{1000}{CN} - 10 \right), \tag{8}$$

where S_0 is a scale factor equal to 24.5 mm, for I_a and R measured in millimeters.

Using Equations 6, 7 and 8, the rainfall is converted in runoff through the unique parameter CN for each time step.

The value of CN depends on the soil and on the land cover. The nature of the soil of the basins under analysis were extracted from a soil map produced in 1968 by Orstom agency having a $1/500\,000$. The vegetation cover were derived by the global land cover map released in 2010 by the European Space Agency [38]. In order to estimate the CN parameter for each analyzed catchment, the soil map and the land cover map were superimposed to the watersheds' boundary (see Fig. 11 and Fig. 12). The boundaries of the drained catchments were derived in a GIS environment (JGrass) elaborating the InSAR DEM.

The daily precipitation amount were derived by the three rainfall gauge stations (see Fig. 1) of Ouahigouya ($13°35'N$, $2°26'W$, elevation: 329 m above sea level), Thiou ($13°49'N$, $2°40'W$, elevation: 303 m a.s.l.) and Titao ($13°46'N$, $2°04'W$, elevation: 329 m a.s.l.). The spatial distribution of precipitation was estimated through the inverse distance-squared method [40], in which the estimate of precipitation in location j is given by

$$P_j = \sum_{i=1}^{n} \frac{d_{ij}^{-2} P_i}{\sum_{i=1}^{n} d_{ij}^{-2}}, \tag{9}$$

where P_i is the measured precipitation at the rainfall gauge i and d_{ij} the distance from gauge i to the location j.

The reservoirs' storage volume was computed on a daily basis through the following water balance:

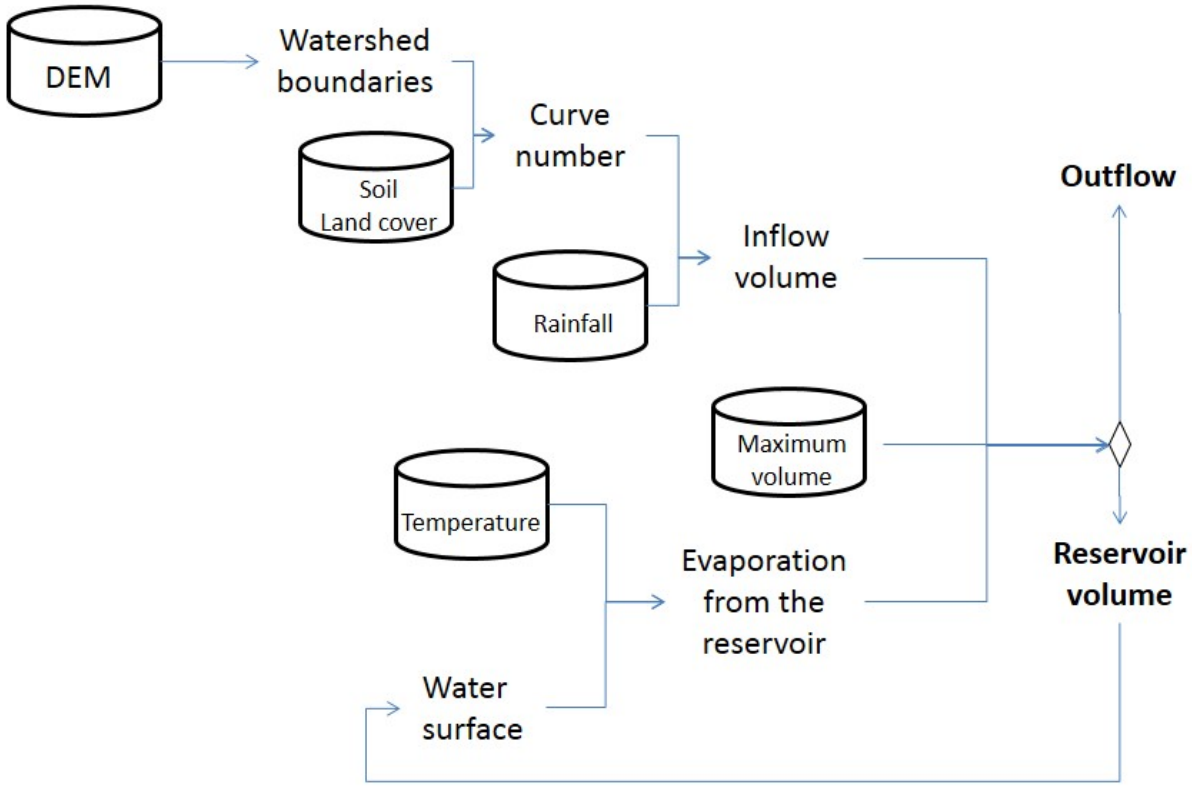

Fig. 10: Block diagram of hydrological model.

$$V_t = \max\left\{V_{t-1} + R_t W - E_t A_{t-1}; V_{\max}\right\}, \tag{10}$$

where V_t is the reservoir storage volume at day t, V_{t-1} is the reservoir storage volume at day $t-1$, R_t is the depth of direct runoff at day t estimated through (6), W is the drained area of the watershed extracted from the DEM, E_t is the depth of evaporation from the reservoir at day t, A_{t-1} is the reservoir surface at day $t-1$ and $V_{\max}$ is the maximum reservoir capacity. In the absence of records about water withdrawal from the reservoir, this term has been neglected in the balance. As a consequence the modelling results will overestimate the reservoir storage in the dry season, that is typically the period in which the water is extracted.

The simulation is iterative. The volume at time t is computed from the value at time $t-1$. The initial condition is, for each year, the water volume estimated by SAR acquisitions at the end of the dry season. However, in order to run the model, the estimation of the unknowns E_t, A_{t-1} and $V_{\max}$ is necessary.

As for the estimation of E_t, since local measurements of net radiation or fractional cloud cover are not available, a temperature-based model has been implemented using the daily temperature measurements at Ouahigouya station in the Hargreaves equation [40]:

$$E_t = 0.0023 E_0 \delta_T \left(T_t + 17.8\right) \text{ [mm/day]}, \tag{11}$$

where T_t is the temperature at time t in Celsius degrees, δ_T is the difference between mean monthly maximum and minimum temperatures and E_0 is the water equivalent of extraterrestrial radiation in $[mm/day]$ for the location of interest computed as follows:

$$E_0 = 15.392 d_r \left(\omega_s \sin\phi \sin\delta + \cos\phi \cos\delta \sin\omega_s\right), \tag{12}$$

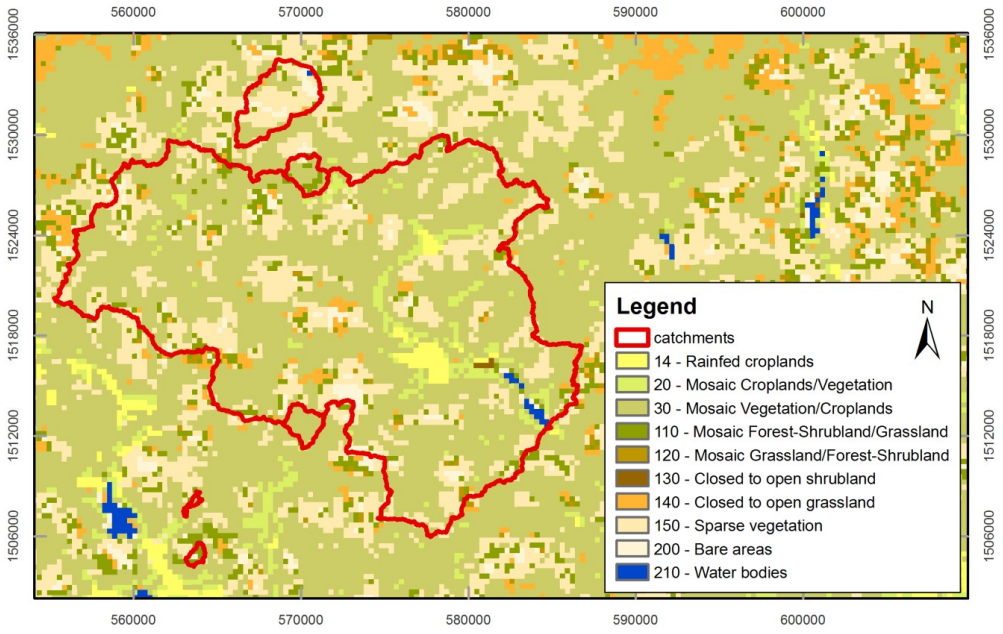

Fig. 11: Watershed boundaries superimposed to land cover map.

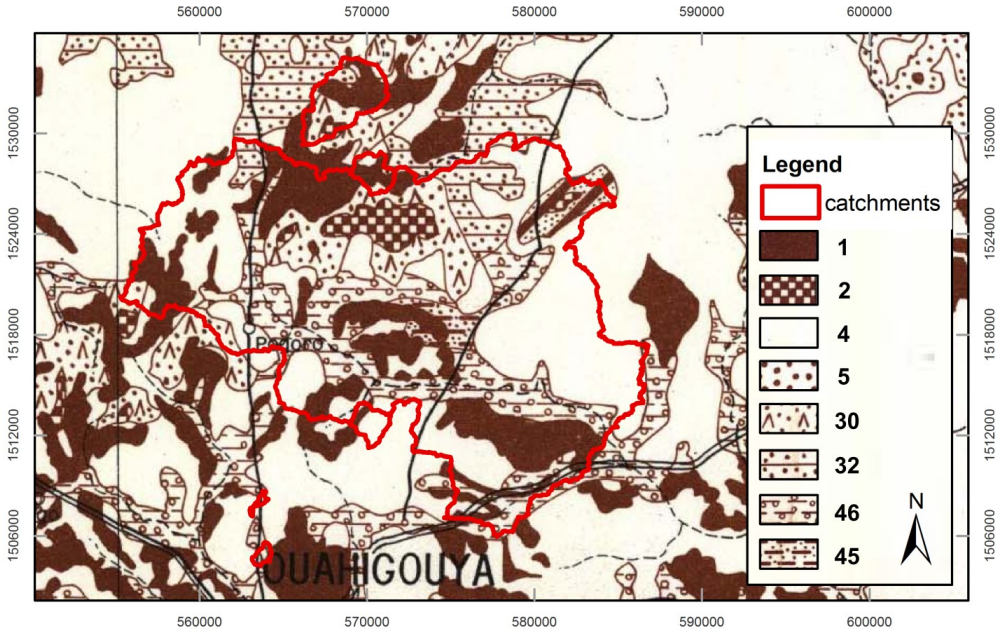

Fig. 12: Pedological map of Haute-Volta (Centre North). 1. Sur cuirasse ferrugineuse; 2. Sur roches diverses; 3. Association lithosals sur cuirasse ferrugineuse; 5. Association sols ferrugineux lessivs (ou appauvris) sur matriau argilo-sableux; 30. Association sols bruns eutrophes sur matrieu argileux issu de roches basiques; 32. Association sols hydromorphes sur matriau argileux issu de schistes argileux (BIRRIMIEN); 45. Association sols bruns eutrophes sur matrieu argileux et sols ferrugineux peu lessivs su sables oliens ou sur sables fins argileux; 46. Association sols ferrugineux peu lessivs sur matrieu sablo-argileux peu pais niveau gravillonaire (source [39]).

in which ϕ is the latitude, δ the solar declination in radians, ω_s the sunset hour angle in radians and d_r the relative distance between the earth and the sun. These quantities can be computed as follows:

$$\delta = 0.4093 \sin\left(\frac{2\pi}{365} J - 1.405\right) \tag{13}$$

$$\omega_s = \arccos\left(-\tan\phi \tan\delta\right) \tag{14}$$

$$d_r = 1 + 0.0033 \cos\left(\frac{2\pi}{365} J\right), \tag{15}$$

where J is the Julian day number.

The water area of reservoirs A_{t-1} is computed depending on the volume at time $t-1$, i.e. V_{t-1}. To this end, an empirical equation is derived, for each basin through linear regression of the volume-surface series obtained from the DEM analysis. The estimation is performed at time step $t-1$ in order to make the procedure explicit.

The maximum reservoir capacity $V_{\max}$ is assumed to be equal to the maximum observed volume. This assumption does not hold if the reservoir does not fill up completely at least once in the observation period. However, it is of course realistic since the small reservoirs under study are usually at their maximum capacity for long periods in the year.

Reservoirs' retention volumes estimated through (10) were compared with those calculated from SAR images (see Fig. 13). Although the extreme simplicity of the model, the absence of calibration and the neglecting of the water withdrawal from the reservoir, the agreement is quite good for almost all the studied catchments. In fact, only the simulation relevant to the Tougou basin is rather disappointing. This is probably due to the bigger dimensions of this watershed with respect to the others and to the presence of other water retention basins in its catchment area, which influence the discharge regime at the outlet.

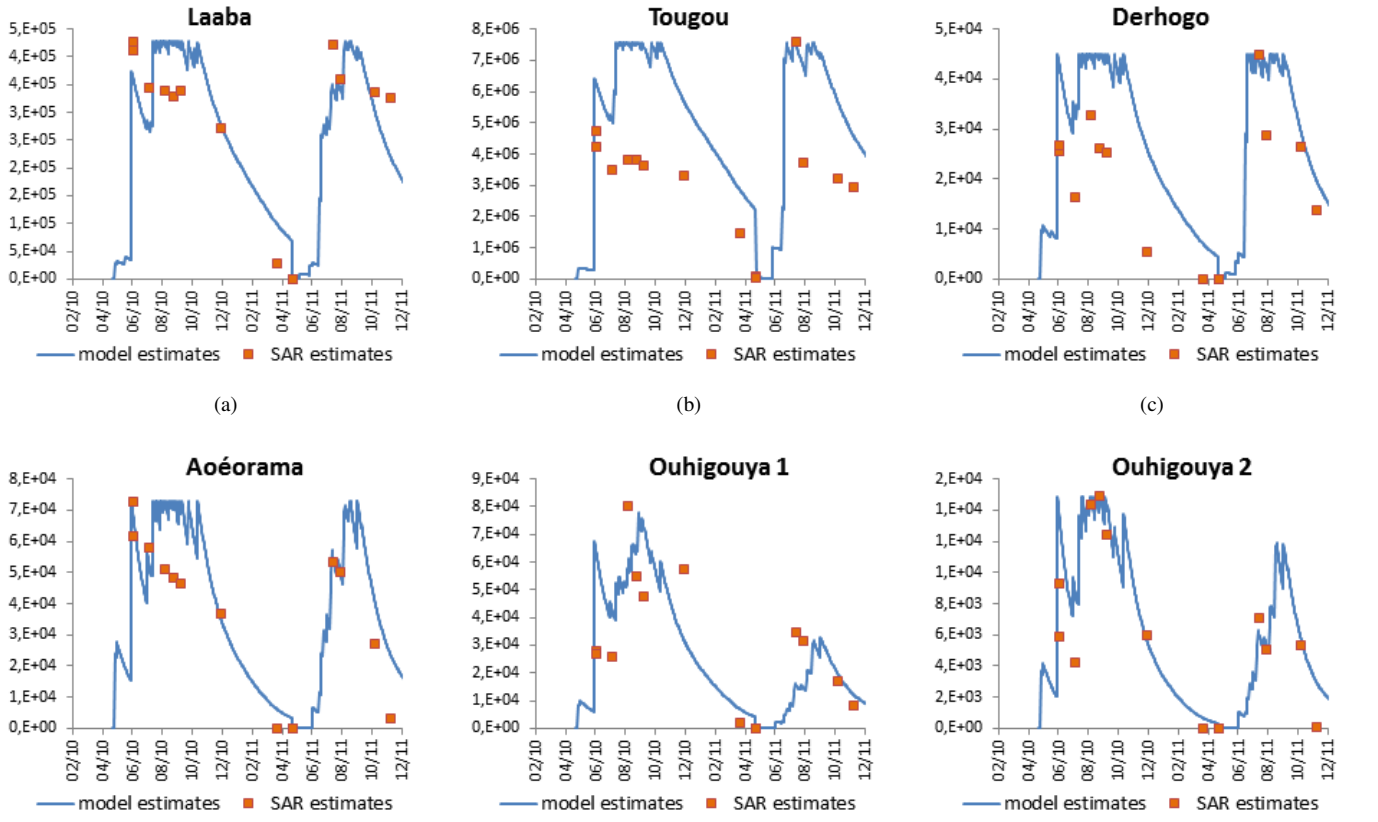

Fig. 13: Simulated retention volumes (m^3) compared to the ones extracted by SAR images.

The model fits quite well the hydrological behavior of the smallest watersheds as Ouahigouya 2 (0.4 km^2) and Ouahigouya 1 (0.9 km^2), catches the behaviour of the small ones, i.e. Aoérama (3.7 km^2) and Derhogo (4 km^2), while the prediction capability resulted to be worst for the bigger basins of Laaba (15.5 km^2) and Tougou (411 km^2). Although the assumptions made and the uncertainties linked to the estimation of some of the input data, the model is able to catch the overall behavior of the system and therefore can be used for the simulation of different scenarios of water management. The agreement in the dry season is also quite good; this is probably due to the fact that the amount of extracted water is small compared to the big amount of water lost for evaporation.

In some cases the water storage simulated in the rainy season are greater than the ones extracted by the SAR data. This discrepancy could be due to the fact that, after the beginning of the rainy season, the vegetation grows at boundaries of the artificial lakes, making it difficult to recognize precisely the shoreline from the SAR images.

C. Possible applications and benefits of integrated modeling

The model proposed can be used to improve the efficiency of the reservoir management. As an example, three different scenarios of water abstraction are simulated for the Laaba basin. In the first scenario, it is assumed that the irrigation abstraction is uniformly distributed in six months; in the second scenario the abstraction is concentrated in four months, and in the third in three months. The efficiency of the system is estimated by the ratio c_i between the the water volumes used for irrigation and the total water volume which enters into the reservoir as runoff flow in one year, i.e. between May 2010 to April 2011. As shown in TABLE II, the system is more efficient when the abstraction of irrigation water is concentrated in a short period immediately successive to the end of the rainy season. For example, if the abstraction is concentrated in three months, it is possible to use the 53% of the total inflow volume into the reservoir, while, if the abstraction is diluted in six months, only the 23% can be used. This is due to the fact that the longer the water is retained in the reservoir the bigger the loss of water for evaporation will be. In the simple examples showed we assessed only the total abstracted volume, but the real variables to maximize are the crop production and the economic benefits for the community. These variables can be computed by the model after introducing agronomic and economic parameters. In this way it would be possible to use the model for the optimization of the regulation strategy of the reservoirs.

TABLE II: Laaba basin efficiency for three different management scenarios.

	Scenario 1	Scenario 3	Scenario 3
Number of months of irrigation abstraction	6	4	3
Total amount of abstraction $[m^3]$	321300	590400	797657
Total amount of evaporation $[m^3]$	684851	668097	585304
c_i	23%	42%	56%
c_e	48%	47%	41%

Another important application of the proposed model is the estimation of the impact of small reservoirs on downstream flows. The presence of the reservoirs induce a decrease of the water flow downstream and this is often the reason of social tension between the beneficiaries of the reservoirs and people living downstream along the same river. It is therefore important to estimate the water volumes that are subtracted to the natural flow, because of the presence of the reservoirs. This information is also important in order to allow for equitable sharing and utilization of water resources. The model implemented in this paper can be used to perform such estimate, as shown in TABLE III for the years considered in this study. In the more rainy 2010 all the reservoir overflowed an amount of water between the 17% and 74% of the total incoming flow, while in the drier 2011 the smallest basins did not release volume downstream.

TABLE III: Fraction of the incoming water flow that flowed downstream the dams

Basin	2010	2011
Laaba	51%	13%
Tougouu	67%	12%
Derhogo	74%	48%
Aoérama	73%	48%
Ouahigouya 1	17%	0%
Ouahigouya 2	37%	0%

V. Conclusions

In semiarid regions small reservoirs form a set of well-distributed and easily accessible water sources that are used for agriculture, domestic use, and livestock. Small reservoirs are widely used to reduce the peoples vulnerability to drought and improve their livelihoods.

In order to optimize the management of these reservoirs, the access to information is a crucial problem that calls for cheap, reliable and continuous monitoring. In this paper we propose the use of SAR sensors for extracting meaningful physical parameters and feeding appropriate hydrological models. In particular, the revisit time and the spatial resolution of Cosmo-Skymed data allow a detailed, continuous and wide observation of the territory that deserves to be exploited in regions where in situ measurements are impervious and expensive actions.

We proposed an approach based on the appropriate processing and feature extraction of a set of COSMO-SkyMed stripmap images, devoted to retrieve the presence, extension and volume of small reservoirs in Burkina Faso. An appropriate combination of SAR and hydrological processing led to the realization of a set of products (digital elevation model, surface and volume of small reservoirs, the drained catchment and a rainfall-runoff model) that can be used for hydromorphological characterization of the studied area, reservoir monitoring, water management or prevention and mitigation of conflicts related to water uses. The proposed research intends to contribute to facilitate management practices of the diffuse system of small reservoirs and ensure their sustainable use. Further development of the study are in the direction of improving the input data of the hydrological modelling. For example a better description of the soil and land cover could be obtained by superimposing their classification map over the SAR images or by their estimation from high resolution SAR data, trying also to catch the seasonal change of land cover and soil humidity. In case of availability of longer series of SAR images, after validating the model, the SAR-derived water storages can be assimilated to the model, thus greatly improving its prediction capability.

ACKNOWLEDGMENTS

The authors thank the Direction de la Meteorologie du Burkina Faso for providing the rainfall and temperature measurements of Ouahigouya meteo station and the Salerno and Napoli sections of Engineering Without Borders for supporting the missions of researcher and volunteers in Burkina Faso.

The SAR images, at the basis of the study, were provided by the Italian Space Agency (ASI) under the aegis of the 2007 COSMO-SkyMed AO Project "Use of High Resolution SAR Data for Water Resource Management in Semi Arid Regions".

REFERENCES

[1] E. Boelee, P. Cecchi, and A. Kone, "Health Impacts of Small Reservoirs in Burkina Faso," International Water Management Institute, Colombo, Sri Lanka, IWMI Working Paper 136, 2009.

[2] P. Cecchi, A. Meunier-Nikiema, N. Moiroux, and B. Sanou, "Towards an atlas of lakes and reservoirs in burkina," in *Small reservoir toolkit*, M. Andreini, M. Schuetz, T. Harrington, and L. Battaramulla, Eds. Colombo, Sri Lanka: International Water Management Institute, 2009.

[3] A. Zhang and G. Jia, "Monitoring meterological drought in semiarid regions using multi-sensor microwave remote sensing data," *Remote Sens. Environ.*, vol. 134, pp. 12–23, 2013.

[4] J. Liebe, N. van de Giesen, and M. Andreini, "Estimation of small reservoir storage capacities in semi-arid environment: A case study in the Upper East Region of Ghana," *Phys. Chem. Earth. Pt. A/B/C*, vol. 30, pp. 448–454, 2005.

[5] S. Mutiti, J. Levy, C. Mutiti, and N. S. Gaturu, "Assessing Ground Water Development Potential Using Landsat Imagery," *Ground water*, vol. 48, no. 2, pp. 295–305, 2010.

[6] A. Arledler, P. Castracane, A. Marin, S. Mica, G. Pace, M. Quartulli, G. Vaglio Laurin, I. Alfari, and H. Trebossen, "Detecting water bodies and water related features in the Niger basin area by SAR data: the ESA TIGER WADE project," in *Application of Satellite Remote Sensing to Support Water Resources Management in Africa: Results from the TIGER Initiative*, ser. IHP-VII Technical Documents in Hydrology. Paris: UNESCO, 2010, no. 85.

[7] F. O. Annor, N. van de Giesen, and J. Liebe, "Monitoring of Small Reservoirs Storage Using ENVISAT ASAR and SPOT Imagery in the Upper East Region of Ghana," in *Application of Satellite Remote Sensing to Support Water Resources Management in Africa: Results from the TIGER Initiative*, ser. IHP-VII Technical Documents in Hydrology. Paris: UNESCO, 2010, no. 85.

[8] C. J. Oliver and S. Quegan, *Understanding Synthetic Aperture Radar Images*. Nordwood, MA: Artech House, 1998.

[9] L. Pulvirenti, F. Marzano, N. Pierdicca, S. Mori, and M. Chini, "Discrimination of Water Surfaces, Heavy Rainfall, and Wet Snow Using COSMO-SkyMed Observations of Severe Weather Events," *IEEE Trans. Geosci. Remote Sens.*, vol. 52, no. 2, 2014.

[10] D. O. Nitti, F. Bovenga, R. Nutricato, F. Intini, and M. T. Chiaradia, "On the use of COSMO/SkyMed data and Weather Models for interferometric DEM generation," *European Journal of Remote Sensing*, vol. 46, pp. 250–271, 2013.

[11] J. Liebe, N. van de Giesen, M. Andreini, T. Steenhuis, and M. Walter, "Suitability and Limitations of ENVISAT ASAR for Monitoring Small Reservoirs in a Semiarid Area," *IEEE Trans. Geosci. Remote Sens.*, vol. 47, no. 5, pp. 1536–1547, 2009.

[12] M. Koch, T. Schmid, M. Reyes, and J. Gumuzzio, "Evaluating Full Polarimetric C- and L-Band Data for Mapping Wetland Conditions in a Semi-Arid Environment in Central Spain," *IEEE J. Sel. Topics Appl. Earth Observ.*, vol. 5, no. 3, pp. 1033–1043, 2012.

[13] D. Amitrano, G. Di Martino, A. Iodice, D. Riccio, and G. Ruello, "A New Framework for SAR Multitemporal Data RGB Representation: Rationale and Products," *IEEE Trans. Geosci. Remote Sens.*, vol. 53, no. 1, pp. 117–133, 2015.

[14] M. Datcu and K. Seidel, "Human-Centered Concepts for Exploration and Understanding of Earth Observation Images," *IEEE Trans. Geosci. Remote Sens.*, vol. 43, no. 3, pp. 52–59, 2005.

[15] J. Martinez and T. Le Toan, "Mapping of flood dynamics and spatial distribution of vegetation in the Amazon floodplain using multitemporal SAR data," *Remote Sens. Environ.*, vol. 108, no. 3, pp. 209–223, 2007.

[16] N. Tholey, S. Clandillon, and P. De Fraipont, "The contribution of spaceborne SAR and optical data in monitoring flood events: examples in northern and southern France," *Hydrol. Process.*, vol. 11, no. 10, pp. 1409–1413, 1997.

[17] L. Pulvirenti, M. Chini, N. Pierdicca, L. Guerriero, and P. Ferrazzoli, "Flood monitoring using multi-temporal COSMO-SkyMed data: Image segmentation and signature interpretation," *Remote Sens. Environ.*, vol. 115, pp. 990–1002, 2011.

[18] F. O. Annor, N. van de Giesen, J. Liebe, P. van de Zaag, A. Tilmant, and S. N. Odai, "Delineation of Small Reservoirs Using Radar Imagery in a Semi-Arid Environment: A Case Study in the Upper East Region of Ghana," *Phys. Chem. Earth Pt. A/B/C*, vol. 34, no. 4-5, pp. 309–315, 2009.

[19] D. Eilander, F. Annor, L. Iannini, and N. van de Giesen, "Remotely Sensed Monitoring of Small Reservoir Dynamics : A Bayesian Approach," *Remote Sens.*, vol. 6, pp. 1191–1210, 2014.

[20] G. Di Martino, A. Iodice, A. Natale, D. Riccio, G. Ruello, I. Zinno, Y. Koussouben, M. N. Papa, and F. Ciervo, "COSMO-SkyMed AO Projects - Use of High Resolution SAR Data for Water Resource Management in Semi Arid Regions," in *IEEE Int. Geosci. Remote Sens. Symp.*, 2012, pp. 1212–1215.

[21] D. Amitrano, G. Di Martino, A. Iodice, D. Riccio, G. Ruello, M. N. Papa, F. Ciervo, and Y. Koussoube, "Effectiveness of high-resolution SAR for water resource management in low-income semi-arid countries," *Int. J. Remote Sens.*, vol. 35, no. 1, pp. 70–88, 2014.

[22] S. Grimaldi, I. V. Angeluccetti, V. Coviello, and P. Vezza, "Cost-effectiveness of soil and water conservation measures on the catchement sediment budget - The Laaba watershed case study, Burkina Faso," *Land Degrad. Dev.*, 2013.

[23] Agenzia Spaziale Italiana (ASI). COSMO-SkyMed SAR products handbook. [Online]. Available: http://www.cosmo-skymed.it/docs/ASI-CSM-ENG-RS-092-A-CSKSARProductsHandbook.pdf

[24] e geos. COSMO-SkyMed Image Calibration. [Online]. Available: http://www.e-geos.it/products/pdf/COSMO-SkyMed-Image_Calibration.pdf

[25] G. Di Martino, M. Poderico, G. Poggi, D. Riccio, and L. Verdoliva, "Benchmarking Framework for SAR Despeckling," *IEEE Trans. Geosci. Remote Sens.*, vol. 52, no. 3, pp. 1596–1615, 2014.
[26] G. F. De Grandi, M. Leysen, J.-S. Lee, and D. Schuler, "Radar reflectivity estimation using multiple SAR scenes of the same target: technique and applications," in *IEEE Int. Geosci. Remote Sens. Symp.*, 1997, pp. 1047–1050.
[27] J.-S. Lee and I. Jurkevich, "Segmentation of sar images," *IEEE Trans. Geosci. Remote Sens.*, vol. 27, no. 6, pp. 674–680, 1989.
[28] S. G. Dellepiane and E. Angiati, "A New Method for Cross-Normalization and Multitemporal Visualization of SAR Images for the Detection of Flooded Areas," *IEEE Trans. Geosci. Remote Sens.*, vol. 50, no. 7, pp. 2765–2779, 2012.
[29] D. G. Long, R. S. Collyer, and D. V. Arnold, "Dependence of the normalized radar cross section of water waves on Bragg wavelength-wind speed sensitivity," *IEEE Trans. Geosci. Remote Sens.*, vol. 34, no. 3, pp. 656–666, 1996.
[30] F. Braga and L. Tosi and C. Prati and L. Alberotanza, "Shoreline detection: capability of COSMO-SkyMed and high-resolution multispectral images," *European Journal of Remote Sensing*, vol. 46, pp. 837–853, 2013.
[31] D. Amitrano, G. Di Martino, A. Iodice, D. Riccio, G. Ruello, F. Ciervo, M. N. Papa, and Y. Koussoube, "High resolution SAR for the monitoring of reservoirs sedimentation and soil erosion in semi arid regions," in *IEEE Int. Geosci. Remote Sens. Symp.*, 2013, pp. 911–914.
[32] C. Ronse and J. Serra, *Algebraic Foundations of Morphology*, L. Najman and H. Talbot, Eds. Hoboken, NJ: John Wiley & Sons, 2010.
[33] G. Shrivakshan and C. Chandrasekar, "A comparison of various edge detection techniques used in image processing," *International Journal of Computer Science Issues*, vol. 9, no. 5-1, pp. 269–276, 2012.
[34] M. Eineder, "Efficient Simulation of SAR Interferograms of Large Areas and of Rugged Terrain," *IEEE Trans. Geosci. Remote Sens.*, vol. 41, no. 6, pp. 1415–1427, 2003.
[35] V. M. Ponce and R. H. Hawkins, "Runoff curve number: has it reached maturity?" *J. Hydrologic Engrg.*, vol. 1, no. 1, pp. 11–19, 1996.
[36] N. W. Kim and J. Lee, "Temporally weighted average curve number method for daily runoff simulation," *Hydrol. Process.*, vol. 22, p. 49364948, 2008.
[37] E. M. Schneiderman, T. S. Steenhuis, D. J. Thongs, Z. M. Easton, M. S. Zion, A. L. Neal, G. F. Mendoza, and M. Todd Walter, "Incorporating variable source area hydrology into a curve-number-based watershed model," *Hydrol. Process.*, vol. 21, pp. 3420–3430, 2007.
[38] European Space Agency (ESA). GlobCover Land Cover Maps. [Online]. Available: http://due.esrin.esa.int/globcover/
[39] P. Panagos, A. Jones, C. Bosco, and P. S. Senthil Kumar, "European digital archive on soil maps (EuDASM): Preserving importan soil data for public free access," *Int. J. Digital Earth*, vol. 4, no. 5, pp. 434–443, 2011.
[40] D. R. Maidment, *Handbook of hydrology*. McGraw-Hill, 1993.